Environmental Science and Ecotechnology 15 (2023) 100251

Contents lists available at ScienceDirect

Environmental Science and Ecotechnology

journal homepage: www.journals.elsevier.com/environmental-science-and-ecotechnology/

Original Research

Cathodic biofouling control by microbial separators in air-breathing microbial fuel cells

Chao Li, Kexin Yi, Shaogang Hu, Wulin Yang*

College of Environmental Science and Engineering, Peking University, No. 5 Yiheyuan Road, Haidian District, Beijing, 100871, China

ARTICLE INFO

Article history:
Received 14 October 2022
Received in revised form
6 February 2023
Accepted 13 February 2023

Keywords:
Air-breathing MFC
Microbial separator
Niche-selective superiority
Biofouling elimination
Stability and sustainability

ABSTRACT

Microbial fuel cells (MFCs) incorporating air-breathing cathodes have emerged as a promising eco-friendly wastewater treatment technology capable of operating on an energy-free basis. However, the inevitable biofouling of these devices rapidly decreases cathodic catalytic activity and also reduces the stability of MFCs during long-term operation. The present work developed a novel microbial separator for use in air-breathing MFCs that protects cathodic catalytic activity. In these modified devices, microbes preferentially grow on the microbial separator rather than the cathodic surface such that biofouling is prevented. Trials showed that this concept provided low charge transfer and mass diffusion resistance values during the cathodic oxygen reduction reaction of 4.6 ± 1.3 and 17.3 ± 6.8 Ω, respectively, after prolonged operation. The maximum power density was found to be stable at 1.06 ± 0.07 W m^{-2} throughout a long-term test and the chemical oxygen demand removal efficiency was increased to 92% compared with a value of 83% for MFCs exhibiting serious biofouling. In addition, a cathode combined with a microbial separator demonstrated less cross-cathode diffusion of oxygen to the anolyte. This effect indirectly induced the growth of electroactive bacteria and produced higher currents in air-breathing MFCs. Most importantly, the present microbial separator concept enhances both the lifespan and economics of air-breathing MFCs by removing the need to replace or regenerate the cathode during long-term operation. These results indicate that the installation of a microbial separator is an effective means of stabilizing power generation and ensuring the cost-effective performance of air-breathing MFCs intended for future industrial applications.

1. Introduction

Microbial fuel cells (MFCs) represent a new generation of eco-friendly wastewater treatment devices providing simultaneous wastewater treatment and power generation [1,2]. MFCs incorporating air-breathing cathodes were first used to treat wastewater in 2004 and since then have received significant attention in various fields [3,4] with numerous breakthroughs. Zhang et al. [5] proposed the concept of a separator-assembled cathode configuration that was shown to greatly improve performance [5]. Feng et al. [6] demonstrated that a so-called *f* factor was highly correlated with power generation in scaled-up MFCs [6]. Dong et al. [7] suggested a modular design comprising dense stacks that avoided a size effect during MFC scale-up [7]. Research based on the use of microbial electrochemical processes to address environmental issues has also been reported. The devices that have been studied include the microbial electrolysis cell [8], microbial desalination cell [9], microbial carbon capture cell [10] and microbial reverse electrodialysis cell [11,12]. Over the past decade, many landmark studies have also assessed the extracellular electron transport mechanism [13–18], as well as device construction and operational optimization [19–21], innovative material designs [22–24] and functional expansion [25–27]. Several pilot-scale MFC devices having the potential for practical applications have already been reported [28–32]. Thus, MFCs are presently undergoing a transition from laboratory research to practical use, although several remaining challenges still limit further engineering applications.

Air-breathing MFCs have received much attention because they allow energy-free operation [33,34]. However, because the cathodes in these devices are in direct contact with the anolyte, biofouling of the electrode surfaces inevitably occurs during long-term operation [35]. This fouling, in turn, increases the cathodic

* Corresponding author.
E-mail address: wulin.yang@pku.edu.cn (W. Yang).

https://doi.org/10.1016/j.ese.2023.100251

overpotential and decreases the oxygen reduction reaction (ORR) kinetics at the cathode, thus significantly reducing the performance of the MFC [36]. The cathodic biofouling mechanism is now well understood and many mitigation strategies have been developed [36,37]. The most direct approach of physical cleaning is effective in the case of short operational durations but is not helpful during prolonged use because the deposits tend to bond strongly with the cathode and so cannot be fully removed [38]. The *in situ* magnetic cleaning method has been reported to rapidly remove part of the cathodic biofilm [39]. Chemical lysis systems using acids (such as hydrochloric acid or nitric acid) or alkali (such as sodium hydroxide) [40,41] have been found to regenerate cathodes but requires the use of additional chemicals. The use of ultraviolet radiation for cleaning also results in high energy consumption [41]. Specially designed antifouling electrodes, such as those impregnated with antibacterial Ag particles, can alleviate cathodic biofouling but tend to shed Ag particles and present toxicity concerns [42].

The strategies discussed above are primarily meant to control or mitigate biofouling but neglect the positive aspects of the presence of a biofilm layer. As an example, it has been reported that a biofouling layer can decrease the oxygen transfer coefficient at the cathode and limit the diffusion of oxygen into the anolyte [43]. The permeation characteristics of this film can also promote ion transfer inside the MFC, meaning that the biofilm layer acts similarly to a separator membrane [44]. Recently, the concept of a microbial separator was proposed and demonstrated in trials using dual chamber biocathode MFCs. These units were able to restrict the direct diffusion of chemical oxygen demand (COD) in the anode and dissolved oxygen (DO) in the cathode to opposite chambers inside MFCs while exhibiting improved ionic cross-separator transfer performance in the electrolyte [45,46]. On this basis, a microbial separator can be expected to perform similar functions in air-breathing MFCs. Furthermore, a microbial separator may also promote the degradation of pollutants [47]. Thus, it may be important to examine the positive functions of biofouling to allow the further development and application of air-breathing MFCs.

In the present study, the novel concept of a microbial separator in an air-breathing MFC was demonstrated. The current density and power density of such devices were investigated as a means of monitoring stability during prolonged operation. In addition, the migration of oxygen across the cathode with or without the separator (as reflected in transfer coefficients) was determined to quantify the ability of the microbial separator to inhibit oxygen diffusion. Electrochemical impedance spectroscopy (EIS) was also employed to ascertain the effect of the microbial separator on the cathodic ORR while linear sweep voltammetry (LSV) data were acquired to demonstrate stable cathodic catalytic activity. The composition and biodiversity of the biofouling biofilm, the microbial separator and the electroactive biofilm were evaluated based on 16S rDNA high-throughput sequencing. A correlative network analysis, BugBase species phenotype contribution analysis and FAPROTAX function prediction were all employed to establish detailed relationships between microbial characteristics and MFC performance.

2. Materials and methods

2.1. Reactor construction and preparation

In preparation for this work, a number of small-scale 28 mL MFCs were constructed [48]. Carbon fiber brushes were used as anodes along with phase inverted air-breathing cathodes (Fig. 1a), as described in prior papers [24,49]. The microbial separator matrix comprised a small section of nylon fabric (38 mm diameter × 0.25 mm thickness, 1800 PPI) tightly mounted inside

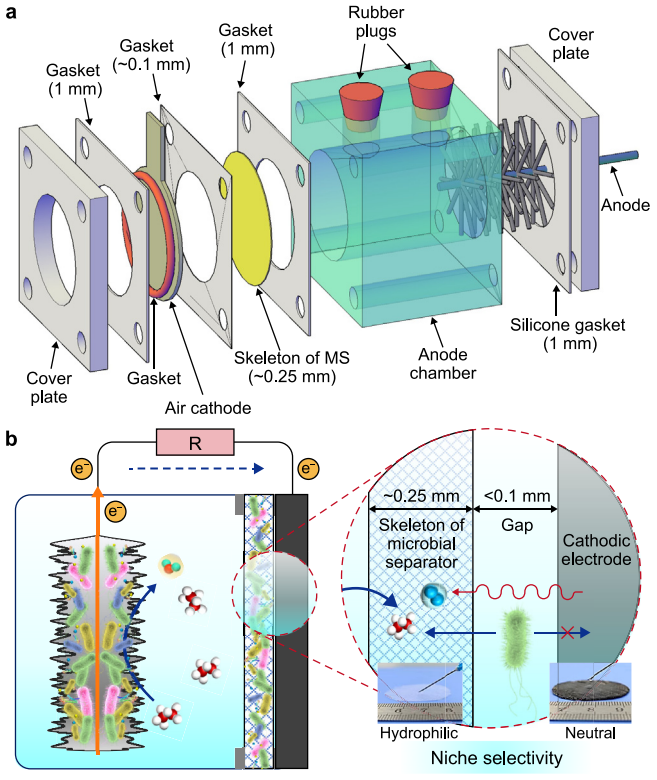

Fig. 1. a, The diagram of a single chamber air-breathing microbial fuel cell installed with microbial separator. **b**, The hypothetical niche-selectivity model in air-breathing MFCs for the biofilm evolution of microbial separator.

the cathode (Fig. 1b). Other details of the reactor design are provided in Fig. 1a. These cubic MFCs were also retrofitted to allow for trials determining the oxygen transfer coefficient ($k_{[DO]}$) (Fig. S1). In this modification process, three holes set at uniform distances were made in the upper part of each device to allow the DO probe, aeration gas vent and PBS solution supply to be attached. An oxygen-degassed needle was installed at a distance of 1 cm from the compartment base and a rotor was used to thoroughly mix oxygen into the solution (Fig. S1). A diagram of the reactor used to evaluate COD transfer coefficient values ($k_{[COD]}$) is presented in Fig. S2. Note that an additional external circulation device was used to stabilize the COD concentration in the bulk solution during the COD diffusion process. The cubic reactor was also modified to assess the ionic conductivity of the test solution before and after the installation of the microbial separator based on acquiring EIS data in a two-electrode system (Fig. S3). During these tests, a high-purity titanium mesh (50 PPI) was used as a counter electrode and a 50 mM phosphate buffered saline (PBS) solution was used as the electrolyte.

2.2. Inoculation and operation

The reactors were inoculated with domestic wastewater and fed with synthetic wastewater containing sodium acetate, trace metals, and vitamins in a batch mode [23]. The experiments were divided into three stages (Fig. 2a). In stage I, parallel reactors were operated for approximately six months to monitor any performance changes in MFCs each having an air-breathing cathode with mature biofouling (referred to herein as the BF stage). In stage II, the cathodes that had undergone biofouling were replaced with fresh cathodes (representing the FC stage) and the MFCs were

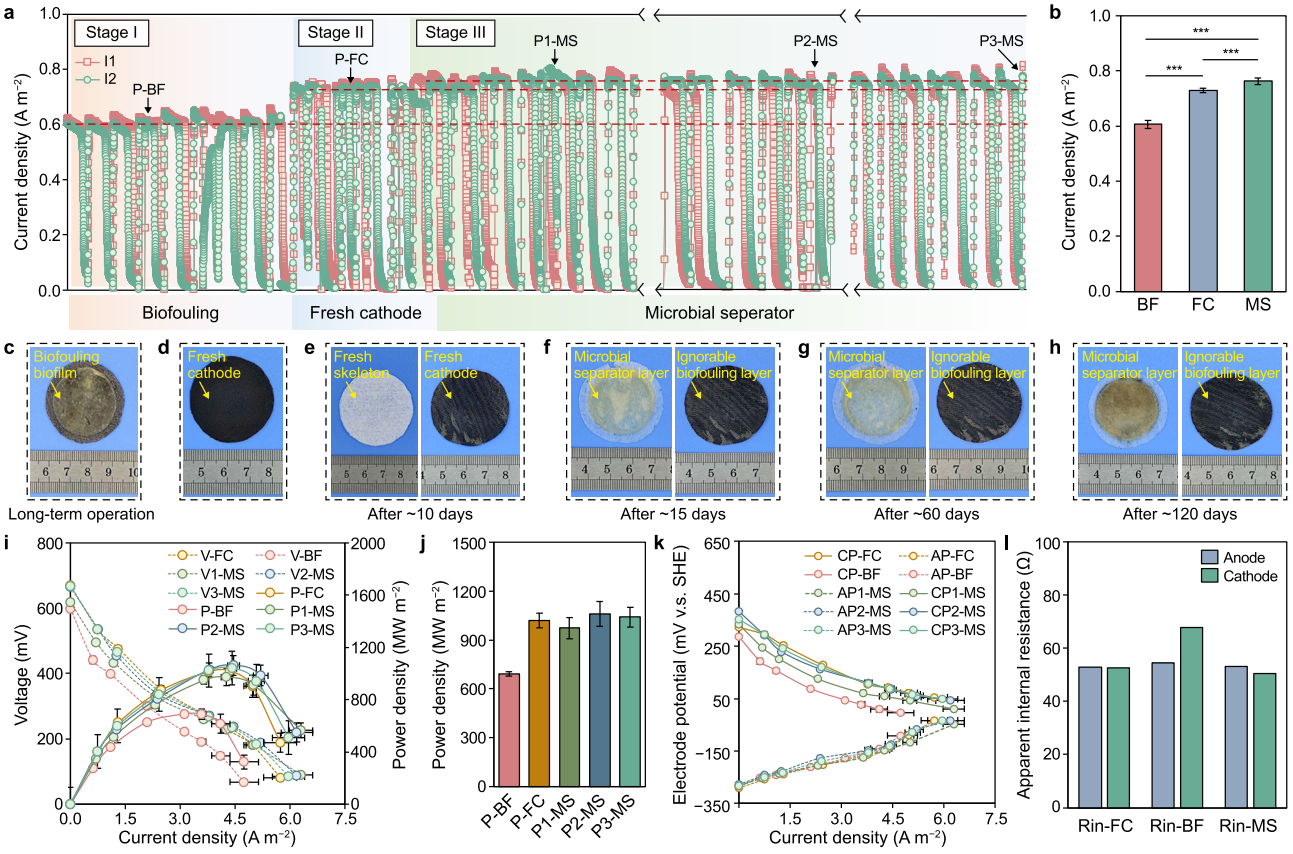

Fig. 2. **a**, The output current density of air-breathing MFCs without or with microbial separators during long-term operation. **b**, The statistical results of the maximum current density of batch operational mode. **c**, The picture of the cathode with serious biofouling. **d**, The fresh cathode installed in MFCs. **e**, The fresh cathode and fresh skeleton of the microbial separator. **f**–**g**, The biofilm of microbial separator in half a month (**f**) and two months (**g**) development. **h**, The microbial separator with mature biofilm and the cathode with ignorable biofouling after half a year of operation. **i**, The power density and polarization curves. **j**, The maximum power density evolution during the experiment. **k**, The electrode potential curves of MFCs. **l**, The fitting results of apparent internal resistances (R_{in}) of anodic and cathodic electrodes. (BF: MFCs with cathodic biofouling, FC: MFCs with fresh cathodes, MS: MFCs with microbial separator, P: power density, V: voltage, CP: cathode potential, AP: anode potential).

subsequently operated for approximately one week to examine the device performance with fresh cathodes. In stage III, a microbial separator matrix was installed into each MFC along with a fresh cathode and each device was operated for a prolonged time span (the MS stage). During each stage, the output current density curves were recorded and maximum power densities (P_{max}) were obtained as a means of evaluating performance characteristics. In addition, oxygen transfer coefficients were evaluated for a new air-breathing cathode, an air-breathing cathode with biofouling, and an air-breathing cathode combined with a microbial separator. The COD transfer coefficients for the system incorporating a microbial separator with a mature biofilm was also estimated. An analysis based on EIS using the two-electrode method was additionally conducted to evaluate the effect of the microbial separator on ionic conductivity. Data were also acquired during each stage after the system had reached an equilibrium state using a three-electrode technique to ascertain the charge transfer resistance (R_{ct}) and mass diffusion resistance (R_d) values associated with the cathodic reaction. At the end of each stage, microbial samples were acquired from the cathodic biofouling, microbial separator, and anodic electroactive biofilm. Note that all MFCs were operated in a temperature-controlled room at 30 ± 1 °C.

2.3. Measurements and calculation methods

The output voltage (U) of each MFC was recorded via a data acquisition system (DAQ6510, Keithley, USA) with a 5 min sampling interval. The current density (j) was normalized to the unit size in m^2 using the formula $j = U/(R \times S)$, where R is the external resistance and S is the projected area of the cathode electrode (7.1 cm^2). The power density was calculated using the formula $p = U \times j$. Polarization curves were obtained via the gradient reducing resistor method with resistance values of 1000, 510, 220, 100, 75, 51, and 20 Ω and power density curves were subsequently derived and plotted. The apparent internal resistance values (R_{in}) for the various operational conditions were obtained from the slopes of the linear regions of polarization curves around the maximum power output point and the R_{in} of electrodes were calculated from the electrode potential curves. Note that standard deviation values were calculated based on data obtained from trials using duplicate reactors.

The oxygen permeabilities of a new air-breathing cathode, an air-breathing cathode with biofouling, and an air-breathing cathode with a microbial separator were calculated from the stable mass transfer coefficient. This parameter, in turn, was obtained based on the oxygen mass balance in the anodic chamber over time using the equation

$$k = -\frac{V}{At}\ln\left[\frac{C_s - C_t}{C_s}\right], \quad (1)$$

where V is the volume of the anodic chamber (28 mL), A is the working area of the cathode (7.1 cm^2), C_t is the oxygen

concentration in the bulk solution at time t, and C_s is the concentration on the air side of the cathode (assumed to be the saturation concentration of oxygen in water with a value of 7.8 mg L^{-1}) [45,50]. The oxygen concentrations were monitored via a dissolved oxygen probe located at the center of the anodic chamber containing a 50 mM PBS solution, employing a magnetic stirrer to ensure a homogeneous mixture. Prior to each test, the PBS solution was degassed with gaseous nitrogen (99.999%) to removal dissolved oxygen until the DO concentration was below 0.1 mg L^{-1}.

The COD cross-separator transfer coefficients were also estimated based on experiments with a modified reactor and calculated via equation (1) with a C_s value of 780 mg L^{-1}. Charge transfer (R_{ct}) and diffusion resistance (R_d) values associated with the cathodic ORR were determined from EIS data collected with an electrochemical workstation (VSP-3e, Bio-logic, USA). During these tests, the cathode acted as the working electrode (WE), the bioanode was the counter electrode (CE) and a saturated calomel reference electrode (SCE, +241.5 mV versus standard hydrogen electrode, SHE) was employed as the reference electrode (RE). The frequency of sinusoidal perturbations during these trials ranged from 100 kHz to 10 mHz with a 10 mV amplitude at the cathodic working potential. The ionic conductivity of the microbial separator as reflected by the ohmic resistance (R_s) was also evaluated based on EIS data. The composition and biodiversity of each microbial sample, including those associated with cathodic biofouling, the microbial separator and the anodic electroactive biofilm, was analyzed using a 16S rDNA high-throughput sequencing method (Shanghai Majorbio Bio-pharm Technology Co., Ltd. and its cloud platform) [51].

3. Results and discussions

3.1. Effect of a microbial separator on long-term stability

A separator is typically employed in a dual-chamber rather than a single-chamber MFC. In the case of air-breathing MFCs, the cathode works to close the MFC circuit and can be considered as a compressed cathode chamber. This configuration reduces the apparent internal resistance (R_{in}) of the dual-chamber MFC by 50%. However, cathodic biofouling is inevitable when the electrode is in direct contact with the anolyte. In the work reported herein, the air-breathing cathode was covered with a thick biofilm after six months of operation, such that the maximum current density (I_{max}) obtained from the MFC was decreased to 0.61 ± 0.02 A m^{-2} (Fig. 2a–c). The installation of a fresh cathode (Fig. 2d) immediately increased I_{max} to 0.73 ± 0.01 A m^{-2} (Fig. 2b), indicating the significant effect of cathodic biofouling on MFC performance. The maximum power density was 0.69 ± 0.02 W m^{-2} after biofouling but 1.02 ± 0.04 W m^{-2} with a fresh cathode (Fig. 2i, j). The apparent internal resistance value (R_{in}) for the cathode was approximately 15.1 Ω after fouling but no obvious changes were observed in the value for the anode (Fig. 2k, l). In subsequent trials, a microbial separator matrix was installed inside a new cathode (Fig. 2e) and there were no significant changes in output current density or apparent internal resistance (Fig. 2b, l). After approximately two weeks, a biofilm had been grown on this separator (Fig. 2f) and the highest current density (I_{max}) was maintained at approximately 0.76 ± 0.01 A m^{-2} (Fig. 2a, b). More importantly, the mature biofilm was found to have grown selectively on the separator skeleton rather than on the cathode (Fig. 2g, h) after six months' operation, even though the microbial separator and cathode were in close proximity to one another. This phenomenon completely eliminated the biofouling of the air-breathing MFCs. During long-term operation for approximately six months, the P_{max} values of MFCs with microbial separators and air-breathing cathodes remained stable at 1.02 ± 0.03 W m^{-2} (Fig. 2j) while the cathodic R_{in} remained low at 50.5 Ω (Fig. 2l). It is of note that LSV analyses also indicated that the cathodic catalytic activity was maintained (Fig. S4). The response current obtained from the microbial separator reached a value of approximately 40 mA at a potential of −1.0 V after six months of operation, equal to twice the value observed after biofouling. The coulombic efficiency (CE) and coulombic recovery (CR) of the MFCs with microbial separators were determined to be 24.5% and 26.7%, respectively, and so were much higher than the values of 16.8% and 20.4% for the devices showing serious cathodic biofouling. Therefore, the microbial separator appears to have completely eliminated rather than simply reduced cathode biofouling in these devices to ensure the long-term stability of air-breathing MFCs.

3.2. Restricted cross-cathode transfer of oxygen

The stability of MFCs incorporating air-breathing cathodes is greatly affected by the use of an anaerobic anolyte and an efficient cathodic ORR rate. The ideal separator for an MFC should restriction oxygen and COD diffusion while maintaining the cross-separator transfer of ions [52]. In the present study, the $k_{[COD]}$ for the microbial separator was determined to be approximately 7.5 × 10^{-6} cm s^{-1} (Fig. S5). Although this value was much higher than those obtained using ion-selective membranes (Table 1), this result suggests that the cross-separator transfer of COD could be inhibited [45]. In addition, the $k_{[DO]}$ of a fresh cathode without biofouling was found to be (1.000 ± 0.003) × 10^{-3} cm s^{-1} (Fig. 3a) such that the anodic DO concentration was 0.86 ± 0.21 mg L^{-1}. Oxygen diffusing into the anolyte has been found to compete with exoelectrogenic bacteria for electrons to limit the generation of current in MFCs [36]. Prior research has attempted to optimize the electrodes in these devices to balance the amount of oxygen migrating into the anolyte with that reacting during the cathodic ORR [50]. In the work reported herein, the presence of a thick biofilm on the cathodic electrode caused the $k_{[DO]}$ value to rapidly drop to (7.1 ± 0.1) × 10^{-5} cm s^{-1} (Fig. 3a) while the DO concentration in the anolyte was also low at 0.64 ± 0.17 mg L^{-1} (Fig. 3b). Under these conditions, the maximum power density was reduced by approximately 32% because the biofouling significantly lowered the cathodic catalytic activity (Fig. 3b). However, a microbial separator covered with a mature biofilm was determined to also inhibit oxygen diffusion. Specifically, an oxygen transfer coefficient of (1.63 ± 0.02) × 10^{-4} cm s^{-1} was obtained (Fig. 3a). This value was equal to those observed using ion-selective membranes (Table 1). The microbial separators also maintained the DO concentration in the anolyte below 0.66 ± 0.08 mg L^{-1} (Fig. 3b). In sharp contrast, the biofouling that caused cathodic deactivation was completely avoided in the case that bacteria were directionally enriched at the oxic/anoxic interface of the microbial separator between the air-breathing cathode and anolyte (Fig. 2f–h). In fact, this interface was a favorable environment for the growth of mixed microbes [62]. In addition, the microbes in the microbial separator had preferential access to the substrate, thus allowing niche-selective growth (Fig. 1b) such that the output P_{max} was comparable to those of MFCs with fresh cathodes.

Analyses based on EIS were employed to characterize ionic transfer inside the MFCs as well as the extent of charge transfer and mass diffusion during the cathodic ORR (Fig. 3c). The anolyte ionic transfer value (R_s) was not impacted by the installation of a microbial separator (Fig. 3g, Table 1) and the separator was found to be beneficial in terms of providing improved permeability and a lack of ion selectivity [45]. The charge transfer resistance (R_{ct}) and mass diffusion resistance (R_d) values were also evaluated and demonstrated the positive effects of a microbial separator on the cathodic ORR. In the case of an MFC incorporating a new cathode,

Table 1
The comparison of key parameters between various separators and microbial separator.

Separator	Oxygen transfer coefficient ($\times 10^{-4}$ cm s^{-1})	COD transfer coefficient ($\times 10^{-4}$ cm s^{-1})	Internal resistance (Ω)	Cost (USD m^{-2})	Reference
PEM	6.7	2.2	93 ± 2	1400	[53,54]
J-cloth	29	-	-	400	[52]
Nafion	1.3	0.00043	84 ± 2	400[a]	[53,54]
UFM	0.19	0.000089	4779	350	[54,55]
CEM	0.94	0.00014	84 ± 2	200	[54]
AEM	0.94	0.00055	88 ± 4	80	[52,54]
Zirfon	19	-	2727	45[a]	[56,57]
Earthenware	-	-	-	5[a]	[58]
Non-woven cloth	-	-	37–51	2–4	[53,59]
EPS	2.7	-	500	1.3[a]	[60]
Glass fiber	0.5	-	2.2	0.31	[55,61]
Microbial separator	1.63 ± 0.02	0.075	~0.3	0.2	This study

Abbreviations: PEM, Proton exchange membrane; UFM, Ultrafiltration membrane; CEM, Cation exchange membrane; AEM, Anion exchange membrane; EPS, Expanded polystyrene.
[a] Calculated or extrapolated from the original research.

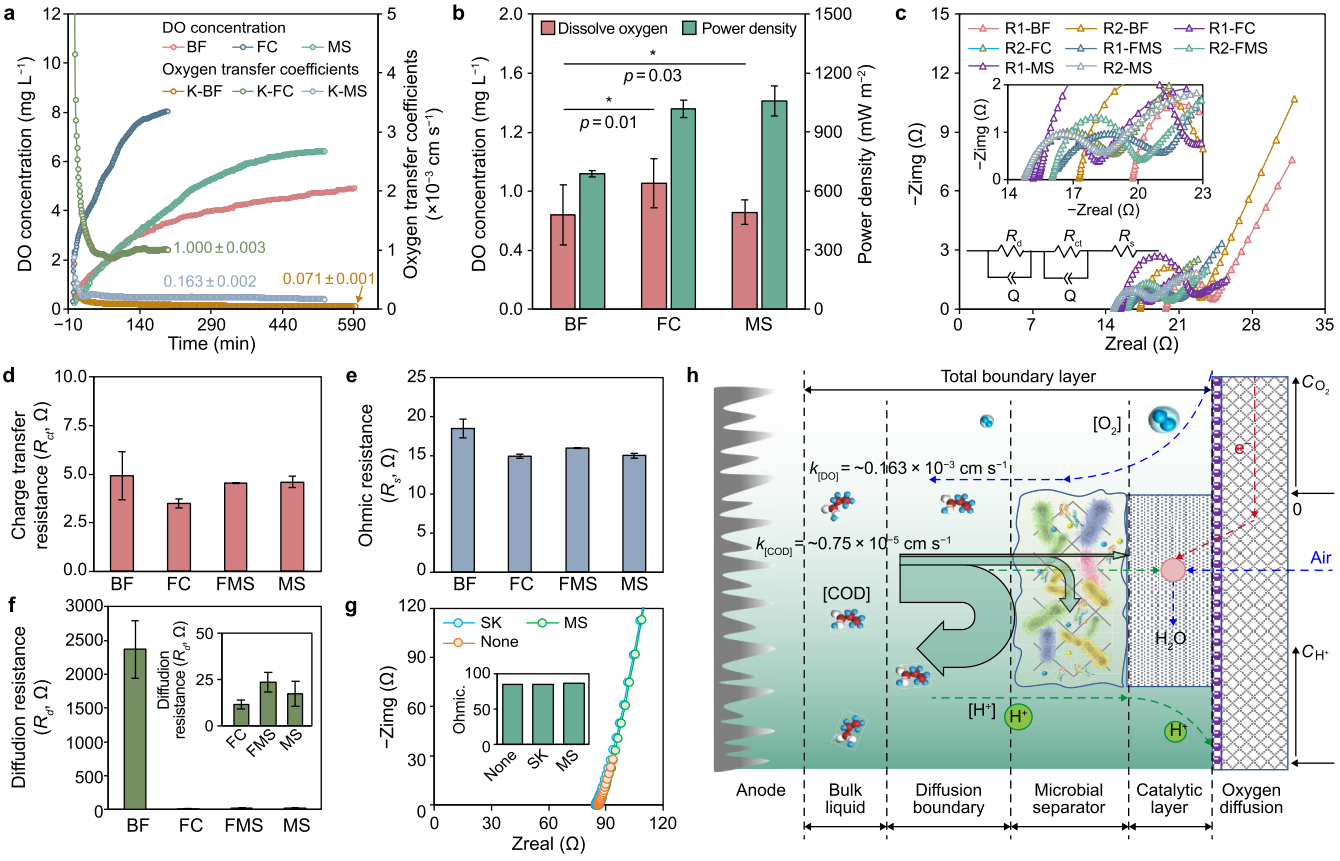

Fig. 3. **a**, The dissolved oxygen transfer coefficients of the cathode with biofouling (BF), fresh cathode (FC), and cathode assembled with microbial separator (MS). **b**, The response of maximum power density to anodic DO concentrations under various conditions. **c**, The electrochemical impedance spectroscopy (EIS) analysis for the cathodic reduction reaction (The inserted image is a partial enlargement of the original image). **d**–**e**, The fitting results of the charge transfer resistances (R_{ct}, **d**), the solution resistances (R_s, **e**). **f**, The mass diffusion resistances (R_d) in EIS analysis (The inserted image is a partial enlargement of the original image). **g**, The ionic conductivity testing results (inserted image) of the microbial separator represented by ohmic resistances. **h**, The schematic diagram of microbial separator model in air-breathing MFCs. (FC: fresh cathode, BF: cathode with biofouling, MS: microbial separator with mature biofilm, FMS: fresh microbial separator in development, SK: the skeleton of microbial separator, RX: reactor X).

the R_{ct} and R_d for the cathodic ORR were 3.5 ± 0.6 and 11 ± 2 Ω, respectively (Fig. 3d, f) but these values rapidly increased to 4.9 ± 0.7 and 2369 ± 424 Ω when the cathode was subjected to a high level of biofouling (Fig. 3d, f). Biofouling also increased the solution resistance (R_s) from 14.9 ± 0.2 Ω with a fresh cathode to 18.5 ± 1.2 Ω after fouling (Fig. 3e). In contrast, during a prolonged trial incorporating a mature microbial separator, the R_{ct} and R_d associated with the ORR were both low and relatively constant at approximately 4.6 ± 1.3 and 17.3 ± 6.8 Ω (Fig. 3d, f). These results indicate that the separator worked to maintain cathodic catalytic activity. In summary, a mature microbial separator allowed each air-breathing MFC to generate high currents by maintaining

catalytic activity during the cathodic ORR (Fig. 3h).

3.3. Enhanced electroactive anodic biofilm growth

The biodiversity and microbial compositions of the microbial separators and electroactive anodic biofilms were closely related to the performance of each MFC. Thus, the 16S rDNA sequencing method and associated function prediction analyses were used to establish the correlations between biofilm characteristics and current generation (Fig. 4). The Shannon index values obtained from rarefaction curves showed that the resulting data accurately reflected microbial compositions (Fig. S6a). In addition, a co-occurrence network analysis demonstrated obvious otherness among microbial communities (Fig. S6b). A partial least squares discriminant analysis also confirmed significant classification differences, especially in the case of the separator biofilm and biofouling (Fig. 4a). On the phylum level, Proteobacteria and Actinobacteriota were found to be the dominant species in the biofouling biofilm and the microbial separator communities while Bacteroidota were also common in the biofouling biofilm (Fig. S6c). Desulfobacterota, Bacteroidota, and Proteobacteria were the preponderant phyla in the electroactive anodic biofilms along with numerous bacterial genera undergoing extracellular electron transfer, such as the typical genus *Geobacter* (Desulfobacterota) [14].

A Bugbase phenotypic analysis was employed to assess the

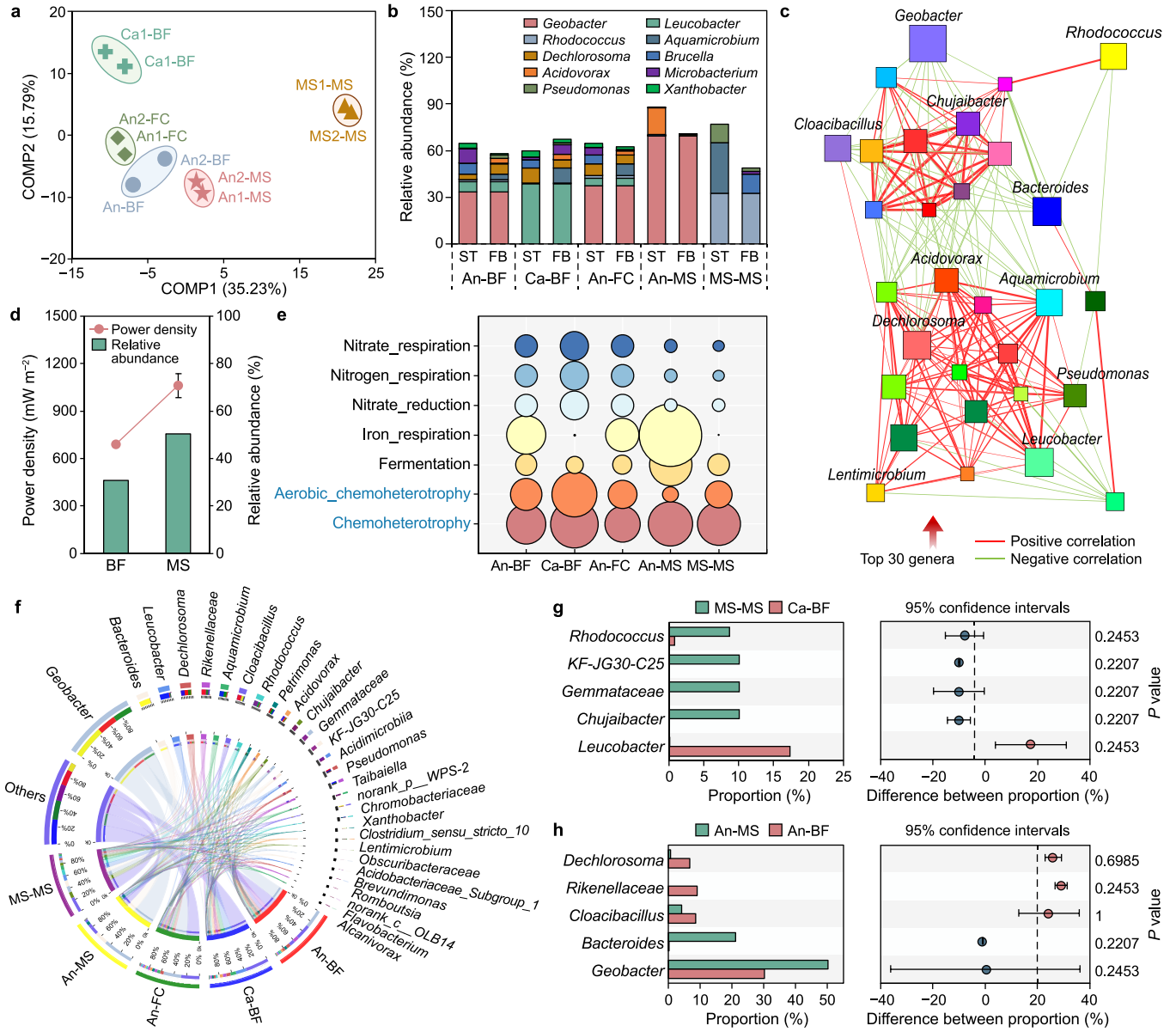

Fig. 4. **a**, The partial least squares discriminant analysis (PLS-DA) of microbial communities. **b**, The Bugbase Phenotypic Prediction and the species-phenotypic contribution analysis in (oxidation) stress tolerant (ST) and forms of biofilm (FB). **c**, The single factor co-occurrence network relationship of top 30 genera. **d**, The response of maximum power density to the relative abundance of *Geobacter* species. **e**, The relative abundance of the functions predicted by FAPROTAX. **f**, The circus map of species to samples on genus level. **g**–**h**, The Wilcoxon rank-sum test bar plots of the biofilm between the microbial separator and cathodic biofouling (**g**) and the anodic samples on genus level (**h**), while the blue and pink circles represent the algebraic difference between a group's data. (FC: fresh cathode, BF: cathode with biofouling, MS: microbial separator with mature biofilm, An: anode, Ca: cathode).

phenotypic properties of the various bacterial communities and to establish the primary species contributing to phenotype expression (Fig. 4b). The relative abundance of functional species contributing to biofilm formation was approximately 50% in the biofilm on the microbial separator (Fig. 4b) and this biofilm included *Rhodococcus*, *Brucella* and others (Fig. 4b). The composition of the biofouling biofilm exhibited obvious otherness, and *Leucobacter* and *Aquamicrobium* were the two dominant genera (Fig. 4b). Although there were large differences in the compositions of the various biofilms, these major phylotypes had similar effects in terms of promoting biofilm development. The microbial separator also promoted directed evolution of anodic electroactive bacteria. In the case of those MFCs exhibiting serious cathodic biofouling, the relative abundance of these bacteria in the anodic biofilm was on the order of 48.1% (Fig. 4f), but increased to 54.6% in MFCs with microbial separators. The particular microbes included *Geobacter*, *Aquamicrobium*, and *Cloacibacillus* among others (Fig. 4f) [14]. In particular, the relative abundance of *Geobacter* rapidly increased to 50.2% in anodic electroactive biofilm in MS stage (An-MS), which was higher than the proportion of 30.2% in the electroactive biofilm in BF stage (An-BF) (Fig. 4d). As reported previously, high current densities in MFCs tend to favor the selective enrichment of electroactive bacteria [23]. In this study, the installation of a microbial separator protected the cathode from biofouling and so maintained the cathodic catalytic activity such that efficient current generation was observed and the quantity of electroactive bacteria was increased.

A correlative network analysis demonstrated a close synergistic relationship between the dominant species in the microbial separator, with the exception of *Geobacter* (Fig. 4c). As an example, the correlation coefficients for the relationships between the most common genera were all greater than 0.5 (Fig. 4c). The FAPROTAX function prediction suggested that the 21 ± 4% of operational taxonomic units (OTUs) in the microbial separators were related to chemoheterotrophy (Fig. 4e), especially for aerobic chemoheterotrophy. This resulted in a favorable anodic habitat with a DO concentration of about 0.66 ± 0.08 mg L^{-1} that was similar to the value observed in devices with serious biofouling (0.64 ± 0.21 mg L^{-1}) (Fig. 3b). A species-phenotypic contribution analysis suggested that *Rhodococcus* and *Romboutsia*, both of which are oxygen-tolerant, were the two dominant genera in the separator biofilms. In addition, *Leucobacter* was the most important genus in terms of contributing to the oxidative stress tolerance of the biofouling biofilms (Fig. 4b). Although there were differences in bacterial abundances, the Wilcoxon rank-sum test on the genus level demonstrated that there was no significant otherness with regard to bacterial biodiversity (Fig. 4g, h). Thus, each of these major phylotypes had a similar effect in terms of restricting cross-biofilm oxygen transfer. Overall, the *in situ* formation of a biofilm on the microbial separator limited the COD and DO cross-separator diffusion and, more importantly, the COD and DO were simultaneously available to the microbial separator rather than the cathode (Fig. 3h). These findings suggest that a microbial separator is superior in terms of realizing the niche-selective enrichment of bacteria and other microbes.

3.4. Improved economics

The economic aspects of next generation devices that are still in the development stage must be carefully evaluated. Thus, to date, several pilot-scale studies have been performed to examine the potential applications of air-breathing MFCs by assessing efficiency and optimization of operation [6,30,32,63,64]. It has been reported that severe cathodic biofouling greatly reduces power density (by approximately 91%) within 77 days [64], such that the replacement or regeneration of cathodes must be conducted within two months. In addition, previous work found that the expense associated with cathodes accounted for 51% of the operating cost of a pilot-scale MFC without expensive cation exchange membrane (CEM) (based on an initial investment of 10,000 USD m^{-3}) [6]. These results demonstrate that the stable and sustainable operation of cathodes would reduce the cost of MFCs by at least half during long-term operation. In this study, very inexpensive nylon textile fabric (approximately 0.2 USD m^{-2}) was employed to fabricate microbial separators (Table 1). Thus, compared with other material reported previously, the present microbial separators are highly economical (Table 1). Consequently, cathodic biofouling was completely avoided and cathodic sustainability was achieved at negligible cost. This practice could therefore eliminate the cost of cathodic regeneration in future pilot-scale equipment during long-term operation.

Stable power generation also improves the economics of air-breathing MFCs. In the present work, a maximum power density of 1.06 ± 0.07 W m^{-2} was obtained from MFCs incorporating microbial separators, which was 35% higher than the value of 0.69 ± 0.02 W m^{-2} for MFCs with serious biofouling. MFCs having higher current densities have been found to promote the growth of electroactive bacteria [65]. The proportional COD removal was also increased from 83% in conjunction with biofouling to 92% when using a microbial separator. It has been suggested that efficient pollutant degradation and lower sludge yields are more important than high coulombic efficiency or power density values during the operation of MFCs [66,67]. In this regard, the biomass formed on the microbial separators was also superior in terms of the extent to which pollutants were removed [66]. As an example, a microbial separator installed in a dual chamber MFC improved COD removal by approximately 8.3% [66] and provided an important pathway for the simultaneous nitrification and denitrification reactions [47]. Although the precise contribution of the microbial separator in an air-breathing cathode MFC to COD removal was not evaluated in this study, it is conceivable that the separator biofilm facilitated the degradation of organic compounds.

3.5. Facile installation of air-cathode MFCs with microbial separators

Energy-free air-breathing MFCs have received spread attention in the wastewater treatment field as more focus has been placed on the efficient use of resources and energy. Over the past decade, several trials of pilot-scale air-breathing MFCs have been reported [6,7,28,30,32], although concerns related to cathodic stability and sustainability continue to limit practical applications. The data acquired using lab-scale MFCs in this work demonstrate the excellent sustainability of cathodes in these devices during long-term operation. On this basis, a potential configuration for a microbial separator unit was proposed for pilot-scale trials, based on multi-module plug-in stacks (Fig. 5). In each module, a single extremely thin porous plate (approximately 0.1 mm) was installed between the microbial separator and cathode to avoid direct contact, while the microbial separator matrix was supported by anolyte pressure (Fig. 5c). Recently, a novel air-breathing cathode capable of withstanding a high pressure (water depth was 13 ± 0.7 m) was reported [49] and this concept was used as the basis for the construction of this novel pilot-scale configuration. This design allowed the fabrication of modular air-breathing cathode MFCs having a plug-in structure that were assembled to build pilot-scale equipment (Fig. 5a, b). As reported, the energy consumed by wastewater treatment plants accounts for close to 3% of the total electrical energy requirement in many municipalities [68]. Thus, a new generation of low-energy microbial electrochemical technology devices would be highly beneficial.

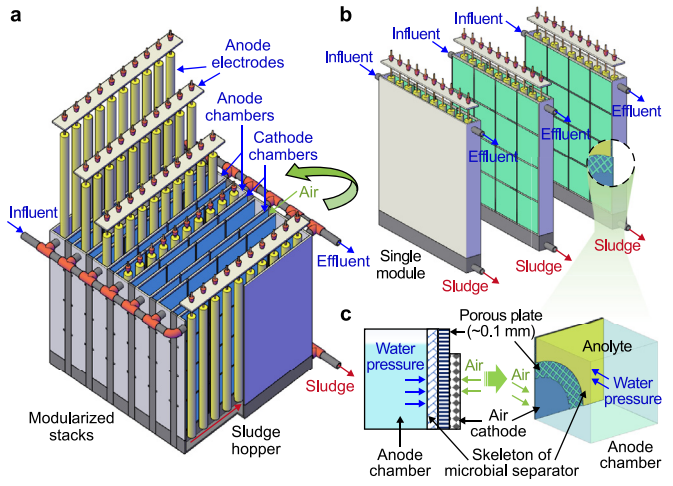

Fig. 5. The schematic structure of a pilot-scale air-breathing microbial fuel cell (MFC) installed with microbial separators. **a**, The schematic of multi-module MFC stacks operated at parallel flow mode. **b**, The schematic of a single module of pilot-scale MFC constructed with multi-panel air-breathing cathode mode (one anode array paired with two cathode arrays), in which the air-breathing cathode is assembled with microbial separator. **c**, The assembly details of 2D side view and 3D section view of separator-cathode design (cathodic electrode, porous plate, and skeleton of microbial separator) installed in the pilot-scale MFC.

4. Conclusion

An innovative design for air-breathing MFCs based on incorporating a microbial separator was demonstrated. During long-term operation, microbes were found to preferentially grow on the microbial separator rather than the cathodic surface as a consequence of niche-selectivity. Microbial separators with mature biofilms effectively blocked the cross-cathode diffusion of oxygen to the anolyte and limited the loss of cathodic catalytic activity. These effects provided a maximum power density as high as 1.02 ± 0.03 W m^{-2}. In addition, these microbial separators showed no negative effects on internal ionic transfer and were found not to be ion selective. Assessments of bacterial biodiversity suggested that the presence of a microbial separator indirectly promoted the growth of an electroactive anodic biofilm while Bugbase phenotypic prediction results demonstrated that the separator biofilm exhibited improved oxygen tolerance. The installation of a microbial separator can greatly improve the sustainability and economics of an air-breathing MFC by removing the need for cathodic replacement or regeneration during prolonged use. The present innovative design employing a microbial separator is evidently an efficient approach to obtaining air-breathing MFCs exhibiting stable power generation and improved removal of pollutants together with lower operational costs and therefore may have future industrial applications.

CRediT authorship contribution statement

Chao Li: Conceptualization, Methodology, Software, Data curation, Writing - original draft preparation. **Kexin Yi:** Visualization, Investigation. **Shaogang Hu:** Supervision, Validation. **Wulin Yang:** Writing - reviewing and editing.

Declaration of competing interest

The authors declare that they have no known competing financial interests or personal relationships that could have appeared to influence the work reported in this paper.

Acknowledgments

This work was supported by the National Nature Science Foundation of China (Grant No. 52100021) and the China Postdoctoral Science Foundation (Grants No. 2022M720004 and No. 2022M710208). The authors appreciated the technical support of the ESE editorial team. Moreover, the first author is deeply grateful to his late grandma (Binxian Tian) and grandpa (Zhiyuan Li).

Appendix A. Supplementary data

Supplementary data to this article can be found online at https://doi.org/10.1016/j.ese.2023.100251.

References

[1] W.W. Li, H.Q. Yu, Z. He, Towards sustainable wastewater treatment by using microbial fuel cells-centered technologies, Energy Environ. Sci. 7 (3) (2014) 911–924.
[2] B.E. Logan, B. Hamelers, R.A. Rozendal, U. Schrorder, J. Keller, S. Freguia, P. Aelterman, W. Verstraete, K. Rabaey, Microbial fuel cells: Methodology and technology, Environ. Sci. Technol. 40 (17) (2006) 5181–5192.
[3] H. Liu, B.E. Logan, Electricity generation using an air-cathode single chamber microbial fuel cell in the presence and absence of a proton exchange membrane, Environ. Sci. Technol. 38 (14) (2004) 4040–4046.
[4] H. Liu, R. Ramnarayanan, B.E. Logan, Production of electricity during wastewater treatment using a single chamber microbial fuel cell, Environ. Sci. Technol. 38 (7) (2004) 2281–2285.
[5] X. Zhang, P. Liang, J. Shi, J. Wei, X. Huang, Using a glass fiber separator in a single-chamber air-cathode microbial fuel cell shortens start-up time and improves anode performance at ambient and mesophilic temperatures, Bioresour. Technol. 130 (2013) 529–535.
[6] Y. Feng, W. He, J. Liu, X. Wang, Y. Qu, N. Ren, A horizontal plug flow and stackable pilot microbial fuel cell for municipal wastewater treatment, Bioresour. Technol. 156 (2014) 132–138.
[7] Y. Dong, Y. Qu, W. He, Y. Du, J. Liu, X. Han, Y. Feng, A 90-liter stackable baffled microbial fuel cell for brewery wastewater treatment based on energy self-sufficient mode, Bioresour. Technol. 195 (2015) 66–72.
[8] D. Call, B.E. Logan, Hydrogen production in a single chamber microbial electrolysis cell lacking a membrane, Environ. Sci. Technol. 42 (9) (2008) 3401–3406.
[9] X. Cao, X. Huang, P. Liang, K. Xiao, Y. Zhou, X. Zhang, B.E. Logan, A new method for water desalination using microbial desalination cells, Environ. Sci. Technol. 43 (18) (2009) 7148–7152.
[10] X. Wang, Y. Feng, J. Liu, H. Lee, C. Li, N. Li, N. Ren, Sequestration of CO2 discharged from anode by algal cathode in microbial carbon capture cells (MCCs), Biosens. Bioelectron. 25 (12) (2010) 2639–2643.
[11] Y. Kim, B.E. Logan, Microbial reverse electrodialysis cells for synergistically enhanced power production, Environ. Sci. Technol. 45 (13) (2011) 5834–5839.
[12] Y. Tian, D. Li, C. Li, J. Liu, J. Wu, G. Liu, Y. Feng, Self-driving CO2-to-formate electro-conversion on Bi film electrode in novel microbial reverse-electrodialysis CO2 reduction cell, Chem. Eng. J. 414 (2021a), 128671.
[13] Y. Gu, V. Srikanth, A.I. Salazar-Morales, R. Jain, J.P. O'Brien, S.M. Yi, R.K. Soni, F.A. Samatey, S.E. Yalcin, N.S. Malvankar, Structure of Geobacter pili reveals secretory rather than nanowire behaviour, Nature 597 (7876) (2021) 430–+.
[14] B.E. Logan, Exoelectrogenic bacteria that power microbial fuel cells, Nat. Rev. Microbiol. 7 (5) (2009) 375–381.
[15] G. Reguera, K.D. McCarthy, T. Mehta, J.S. Nicoll, M.T. Tuominen, D.R. Lovley, Extracellular electron transfer via microbial nanowires, Nature 435 (7045) (2005) 1098–1101.
[16] L. Shi, H. Dong, G. Reguera, H. Beyenal, A. Lu, J. Liu, H.-Q. Yu, J.K. Fredrickson, Extracellular electron transfer mechanisms between microorganisms and minerals, Nat. Rev. Microbiol. 14 (10) (2016) 651–662.
[17] F. Wang, L. Craig, X. Liu, C. Rensing, E.H. Egelman, Microbial nanowires: type IV pili or cytochrome filaments? Trends Microbiol. (2022a) https://doi.org/10.1016/j.tim.2022.11.004.
[18] F. Wang, K. Mustafa, V. Suciu, K. Joshi, C.H. Chan, S. Choi, Z. Su, D. Si, A.I. Hochbaum, E.H. Egelman, D.R. Bond, Cryo-EM structure of an extracellular Geobacter OmcE cytochrome filament reveals tetrahaem packing, Nat. Microbiol. (2022b).
[19] Y. Dong, W. He, D. Liang, C. Li, G. Liu, J. Liu, N. Ren, Y. Feng, Operation strategy of cubic-meter scale microbial electrochemistry system in a municipal wastewater treatment plant, J. Power Sources 441 (2019).
[20] W.H. He, M.J. Wallack, K.Y. Kim, X.Y. Zhang, W.L. Yang, X.P. Zhu, Y.J. Feng, B.E. Logan, The effect of flow modes and electrode combinations on the performance of a multiple module microbial fuel cell installed at wastewater treatment plant, Water Res. 105 (2016) 351–360.
[21] R. Rossi, D. Jones, J. Myung, E. Zikmund, W. Yang, Y.A. Gallego, D. Pant, P.J. Evans, M.A. Page, D.M. Cropek, B.E. Logan, Evaluating a multi-panel air

cathode through electrochemical and biotic tests, Water Res. 148 (2019) 51–59.
[22] H. Dong, H.B. Yu, X. Wang, Q.X. Zhou, J.L. Feng, A novel structure of scalable air-cathode without Nafion and Pt by rolling activated carbon and PTFE as catalyst layer in microbial fuel cells, Water Res. 46 (17) (2012) 5777–5787.
[23] C. Li, Y. Feng, D. Liang, L. Zhang, Y. Tian, R.S. Yadav, W. He, Spatial-type Skeleton Induced Geobacter Enrichment and Tailored Bio-Capacitance of Electroactive Bioanode for Efficient Electron Transfer in Microbial Fuel Cells, Science of the Total Environment, 2022a, 153123.
[24] W. Yang, W. He, F. Zhang, M.A. Hickner, B.E. Logan, Single-step fabrication using a phase inversion method of poly(vinylidene fluoride) (PVDF) activated carbon air cathodes for microbial fuel cells, Environ. Sci. Technol. Lett. 1 (10) (2014) 416–420.
[25] Q. Hu, Y. Ma, G. Ren, B. Zhang, S. Zhou, Water evaporation-induced electricity with Geobacter sulfurreducens biofilms, Sci. Adv. 8 (15) (2022).
[26] Y. Tian, D. Li, G. Liu, C. Li, J. Liu, J. Wu, J. Liu, Y. Feng, Formate production from CO2 electroreduction in a salinity-gradient energy intensified microbial electrochemical system, Bioresour. Technol. 320 (2021b), 124292.
[27] H. Wang, Z.J. Ren, A comprehensive review of microbial electrochemical systems as a platform technology, Biotechnol. Adv. 31 (8) (2013) 1796–1807.
[28] M. Blatter, L. Delabays, C. Furrer, G. Huguenin, C.P. Cachelin, F. Fischer, Stretched 1000-L microbial fuel cell, J. Power Sources 483 (2021), 229130.
[29] W. He, Y. Dong, C. Li, X. Han, G. Liu, J. Liu, Y. Feng, Field tests of cubic-meter scale microbial electrochemical system in a municipal wastewater treatment plant, Water Res. 155 (2019) 372–380.
[30] D.A. Jadhav, I. Das, M.M. Ghangrekar, D. Pant, Moving towards practical applications of microbial fuel cells for sanitation and resource recovery, J. Water Proc. Eng. 38 (2020), 101566.
[31] P. Liang, R. Duan, Y. Jiang, X. Zhang, Y. Qiu, X. Huang, One-year operation of 1000-L modularized microbial fuel cell for municipal wastewater treatment, Water Res. 141 (2018) 1–8.
[32] R. Rossi, A.Y. Hur, M.A. Page, A.O.B. Thomas, J.J. Butkiewicz, D.W. Jones, G. Baek, P.E. Saikaly, D.M. Cropek, B.E. Logan, Pilot scale microbial fuel cells using air cathodes for producing electricity while treating wastewater, Water Res. 215 (2022).
[33] Z. Du, H. Li, T. Gu, A state of the art review on microbial fuel cells: a promising technology for wastewater treatment and bioenergy, Biotechnol. Adv. 25 (5) (2007) 464–482.
[34] C. Santoro, C. Arbizzani, B. Erable, I. Ieropoulos, Microbial fuel cells: from fundamentals to applications. A review, J. Power Sources 356 (2017) 225–244.
[35] P.D. Kiely, G. Rader, J.M. Regan, B.E. Logan, Long-term cathode performance and the microbial communities that develop in microbial fuel cells fed different fermentation endproducts, Bioresour. Technol. 102 (1) (2011) 361–366.
[36] M.T. Noori, M.M. Ghangrekar, C.K. Mukherjee, B. Min, Biofouling effects on the performance of microbial fuel cells and recent advances in biotechnological and chemical strategies for mitigation, Biotechnol. Adv. 37 (8) (2019).
[37] J. Ma, Z. Wang, D. Suor, S. Liu, J. Li, Z. Wu, Temporal variations of cathode performance in air-cathode single-chamber microbial fuel cells with different separators, J. Power Sources 272 (2014) 24–33.
[38] D. Jiang, M. Curtis, E. Troop, K. Scheible, J. McGrath, B. Hu, S. Suib, D. Raymond, B. Li, A pilot-scale study on utilizing multi-anode/cathode microbial fuel cells (MAC MFCs) to enhance the power production in wastewater treatment, Int. J. Hydrogen Energy 36 (1) (2011) 876–884.
[39] R. Rossi, W. Yang, E. Zikmund, D. Pant, B.E. Logan, In situ biofilm removal from air cathodes in microbial fuel cells treating domestic wastewater, Bioresour. Technol. 265 (2018) 200–206.
[40] G. Pasternak, J. Greenman, I. Ieropoulos, Regeneration of the power performance of cathodes affected by biofouling, Appl. Energy 173 (2016) 431–437.
[41] J. Song, L. Liu, Q. Yang, J. Liu, T. Yu, F. Yang, J. Crittenden, PVDF layer as a separator on the solution-side of air-cathodes: the electricity generation, fouling and regeneration, RSC Adv. 5 (65) (2015) 52361–52368.
[42] Y. Dai, Y. Chan, B. Jiang, L. Wang, J. Zou, K. Pang, H. Fu, Bifunctional Ag/Fe/N/C catalysts for enhancing oxygen reduction via cathodic biofilm inhibition in microbial fuel cells, ACS Appl. Mater. Interfaces 8 (11) (2016) 6992–7002.
[43] Z. Wang, G.D. Mahadevan, Y. Wu, F. Zhao, Progress of air-breathing cathode in microbial fuel cells, J. Power Sources 356 (2017) 245–255.
[44] M. Oliot, S. Galier, H.R. de Balmann, A. Bergel, Ion transport in microbial fuel cells: key roles, theory and critical review, Appl. Energy 183 (2016) 1682–1704.
[45] C. Li, W. He, D. Liang, Y. Tian, R. Shankar Yadav, J. Liu, Y. Feng, Power density of microbial electrochemical system responds to mass transfer characters of non–ion–selective microbial separator, Bioresour. Technol. 311 (2020), 123478.
[46] S.J. Liu, Y.J. Feng, J.J. Niu, J. Liu, N. Li, W.H. He, A novel single chamber vertical baffle flow biocathode microbial electrochemical system with microbial separator, Bioresour. Technol. 294 (2019).
[47] C. Li, W. He, D. Liang, Y. Tian, J. Li, Z. Li, Y. Feng, Microbial separator allied biocathode supports simultaneous nitrification and denitrification for nitrogen removal in microbial electrochemical system, Bioresour. Technol. 345 (2022b), 126537.
[48] B. Logan, S. Cheng, V. Watson, G. Estadt, Graphite fiber brush anodes for increased power production in air-cathode microbial fuel cells, Environ. Sci. Technol. 41 (9) (2007) 3341–3346.
[49] K. Yi, W. Yang, B.E. Logan, Defect free rolling phase inversion activated carbon air cathodes for scale-up electrochemical applications, Chem. Eng. J. 454 (2023), 140411.
[50] S. Cheng, H. Liu, B.E. Logan, Increased performance of single-chamber microbial fuel cells using an improved cathode structure, Electrochem. Commun. 8 (3) (2006) 489–494.
[51] C. Li, W. He, D. Liang, Y. Tian, R.S. Yadav, D. Li, J. Liu, Y. Feng, The anaerobic and starving treatment eliminates filamentous bulking and recovers biocathode biocatalytic activity with residual organic loading in microbial electrochemical system, Chem. Eng. J. 404 (2021b).
[52] W.-W. Li, G.-P. Sheng, X.-W. Liu, H.-Q. Yu, Recent advances in the separators for microbial fuel cells, Bioresour. Technol. 102 (1) (2011) 244–252.
[53] S. Choi, J.R. Kim, J. Cha, Y. Kim, G.C. Premier, C. Kim, Enhanced power production of a membrane electrode assembly microbial fuel cell (MFC) using a cost effective poly [2,5-benzimidazole] (ABPBI) impregnated non-woven fabric filter, Bioresour. Technol. 128 (2013) 14–21.
[54] J.R. Kim, S. Cheng, S.-E. Oh, B.E. Logan, Power generation using different cation, anion, and ultrafiltration membranes in microbial fuel cells, Environ. Sci. Technol. 41 (3) (2007) 1004–1009.
[55] X. Li, G. Liu, S. Sun, F. Ma, S. Zhou, J.K. Lee, H. Yao, Power generation in dual chamber microbial fuel cells using dynamic membranes as separators, Energy Convers. Manag. 165 (2018) 488–494.
[56] D. Pant, G. Van Bogaert, M. De Smet, L. Diels, K. Vanbroekhoven, Use of novel permeable membrane and air cathodes in acetate microbial fuel cells, Electrochim. Acta 55 (26) (2010) 7710–7716.
[57] S. Sevda, X. Dominguez-Benetton, K. Vanbroekhoven, T.R. Sreekrishnan, D. Pant, Characterization and comparison of the performance of two different separator types in air-cathode microbial fuel cell treating synthetic wastewater, Chem. Eng. J. 228 (2013) 1–11.
[58] G. Pasternak, J. Greenman, I. Ieropoulos, Comprehensive study on ceramic membranes for low-cost microbial fuel cells, ChemSusChem 9 (1) (2016) 88–96.
[59] S.M. Daud, B.H. Kim, M. Ghasemi, W.R.W. Daud, Separators used in microbial electrochemical technologies: current status and future prospects, Bioresour. Technol. 195 (2015) 170–179.
[60] A.S. Mathuriya, D. Pant, Assessment of expanded polystyrene as a separator in microbial fuel cell, Environ. Technol. 40 (16) (2019) 2052–2061.
[61] D. Sun, B. Xie, J. Li, X. Huang, J. Chen, F. Zhang, A low-cost microbial fuel cell based sensor for in-situ monitoring of dissolved oxygen for over half a year, Biosens. Bioelectron. 220 (2023), 114888.
[62] H. Liu, S. Cheng, L. Huang, B.E. Logan, Scale-Lip of membrane-free single-chamber microbial fuel cells, J. Power Sources 179 (1) (2008) 274–279.
[63] I. Das, M.M. Ghangrekar, R. Satyakam, P. Srivastava, S. Khan, H.N. Pandey, On-site sanitary wastewater treatment system using 720-L stacked microbial fuel cell: case study, J. Hazardous Toxic Radioactive Waste 24 (3) (2020).
[64] H. Hiegemann, T. Littfinski, S. Krimmler, M. Luebken, D. Klein, K.-G. Schmelz, K. Ooms, D. Pant, M. Wichern, Performance and inorganic fouling of a submergible 255 L prototype microbial fuel cell module during continuous long-term operation with real municipal wastewater under practical conditions, Bioresour. Technol. 294 (2019).
[65] W. He, W. Jin, Q. Wang, Y. Feng, Electron flow assisted COD removal in wastewater under continuous flow conditions using microbial electrochemical system, Sci. Total Environ. 776 (2021), 145978.
[66] C. Li, W. He, D. Liang, Y. Tian, Z. Li, R.S. Yadav, F. Wang, Y. Yu, Y. Feng, Discerning realizable advantages of microbial electrochemical system towards raw municipal wastewater treatment: from the analyses of mass and energy flow, J. Power Sources 495 (2021a), 229706.
[67] J. Yu, Y. Park, E. Widyaningsih, S. Kim, Y. Kim, T. Lee, Microbial fuel cells: devices for real wastewater treatment, rather than electricity production, Sci. Total Environ. 775 (2021).
[68] P.L. McCarty, J. Bae, J. Kim, Domestic wastewater treatment as a net energy producer-can this be achieved? Environ. Sci. Technol. 45 (17) (2011) 7100–7106.